BJ www.biochemj.org

BJ Cell

Biochem. J. (2009) **419**, 317–328 (Printed in Great Britain) doi:10.1042/BJ20081364

The ABC transporter MsbA interacts with lipid A and amphipathic drugs at different sites

Alena SIARHEYEVA and Frances J. SHAROM[1]

Department of Molecular and Cellular Biology, University of Guelph, Guelph, Ontario, Canada N1G 2W1

MsbA is an essential ABC (ATP-binding cassette) transporter involved in lipid A transport across the cytoplasmic membrane of Gram-negative bacteria. The protein has also been linked to efflux of amphipathic drugs. Purified wild-type MsbA was labelled stoichiometrically with the fluorescent probe MIANS [2-(4′-maleimidylanilino)naphthalene-6-sulfonic acid] on C315, which is located within the intracellular domain connecting transmembrane helix 6 and the nucleotide-binding domain. MsbA–MIANS displayed high ATPase activity, and its folding and stability were unchanged. The initial rate of MsbA labelling by MIANS was reduced in the presence of amphipathic drugs, suggesting that binding of these compounds alters the protein conformation. The fluorescence of MsbA–MIANS was saturably quenched by nucleotides, lipid A and various drugs, and estimates of the K_d values for binding fell in the range of 0.35–10 μM. Lipid A and daunorubicin were able to bind to MsbA–MIANS simultaneously, implying that they occupy different binding sites. The effects of nucleotide and lipid A/daunorubicin binding were additive, and binding was not ordered. The K_d of MsbA for binding lipid A was substantially decreased when the daunorubicin binding site was occupied first, and prior binding of nucleotide also modulated lipid A binding affinity. These results indicate that MsbA contains two substrate-binding sites that communicate with both the nucleotide-binding domain and with each other. One is a high affinity binding site for the physiological substrate, lipid A, and the other site interacts with drugs with comparable affinity. Thus MsbA may function as both a lipid flippase and a multidrug transporter.

Key words: ATP-binding cassette (ABC) superfamily, daunorubicin, fluorescence labelling, lipid A, MsbA, substrate binding.

INTRODUCTION

The ABC (ATP-binding cassette) transporters are a large superfamily of proteins involved in membrane transport of a wide variety of compounds [1–3]. Among their substrates are amphipathic drugs, bile salts, linear and cyclic peptides, steroids, detergents, fluorescent dyes, ionophores and lipids. The prototypical Gram-negative bacterium *Escherichia coli* possesses approx. 80 ABC proteins, accounting for almost 5 % of its genome, most of which are involved in solute import/export. MsbA was initially identified as a membrane-bound ATPase in Gram-negative bacteria that was involved in lipid A export [4–6]. Depletion or loss of function of MsbA results in the accumulation of LPS (lipopolysaccharide) and phospholipids in the cytoplasmic membrane of *E. coli* [4,5,7]. MsbA is thus presumed to translocate lipid A (and possibly certain phospholipids) from the inner to the outer leaflet of the cytoplasmic membrane, although it is not required for phospholipids to reach the outer membrane. However, it has never been directly demonstrated that MsbA is capable of promoting flip-flop of lipids in an ATP-dependent manner [8,9]. Multiple copies of *msbA*-like genes have been identified in many bacterial genomes, whereas lipid A is found only in Gram-negative bacteria, thus suggesting that MsbA might also be involved in the transport of other substrates [6]. MsbA is homologous (~30 % sequence identity) to bacterial LmrA from *Lactococcus lactis* and human Pgp (P-glycoprotein; ABCB1), both of which are drug efflux pumps causing MDR (multidrug resistance) [10,11], and functional studies in intact cells suggest that it can also transport multiple drugs [12,13]. LmrA can functionally substitute for a temperature-sensitive MsbA mutant in *E. coli* WD2 at non-permissive temperatures [12], and when expressed in *L. lactis,* MsbA confers resistance to certain antibiotics, and displays Hoechst 33342 and ethidium transport that can be inhibited by lipid A and vinblastine [13].

MsbA is a ‘half-transporter’, comprising a TM (transmembrane) domain with 6 membrane-spanning helices, which are believed to contain the substrate-binding site, and a NBD (nucleotide-binding domain), for a total molecular mass of 64.5 kDa [4–7] (Figure 1A). The functional MsbA transporter is presumed to be a homodimer. Substrate transport is driven by the energy provided by ATP hydrolysis, therefore interaction between the NBDs and the TM domains is essential. Purified MsbA displays basal ATPase activity that can be modulated by phospholipids and a variety of lipid A species [7,14].

Following the retraction of high resolution X-ray crystallographic structures of three closely-related MsbA orthologues, reinterpreted structural models based on the original data appeared recently [15]. The structure of *Salmonella typhimurium* MsbA with bound nucleotide shows a close association of the two NBDs to form a ‘sandwich dimer’ of the type previously observed for other isolated NBD subunits [16,17] and intact prokaryotic ABC transporters [18–20], and may represent a ‘closed’ inward-facing conformation. The six TM helices in each MsbA monomer extend into the cytosol, forming an ICD (intracellular domain) that may play a role in coupling ATP hydrolysis to substrate transport. In contrast, the 5.3 Å (1 Å = 0.1 nm) resolution structure of *E. coli* MsbA in the absence of nucleotide shows a 50 Å separation between the NBDs of the two monomers, and was proposed to represent an “open” inward-facing conformation of the transporter. However, it is possible that this atypical dimeric structure represents a crystallization artefact, since it seems unlikely that an ABC protein would undergo such a large movement during each catalytic cycle.

Abbreviations used: ABC, ATP-binding cassette; ATP[S], adenosine 5′-[γ-thio]triphosphate; DM, *n*-dodecyl-β-D-maltoside; DTE, dithioerythritol; ICD, intracellular domain; MALDI–TOF, matrix-assisted laser-desorption ionization–time-of-flight; MDR, multidrug resistant/resistance; MIANS, 2-(4′-maleimidylanilino)naphthalene-6-sulfonic acid; NBD, nucleotide-binding domain; Ni-NTA, Ni^{2+}-nitrilotriacetate; PC, phosphatidylcholine; Pgp, P-glycoprotein; p[NH]ppA, adenosine 5′-[β,γ-imido]triphosphate; TM, transmembrane.

[1] To whom correspondence should be addressed (email fsharom@uoguelph.ca).

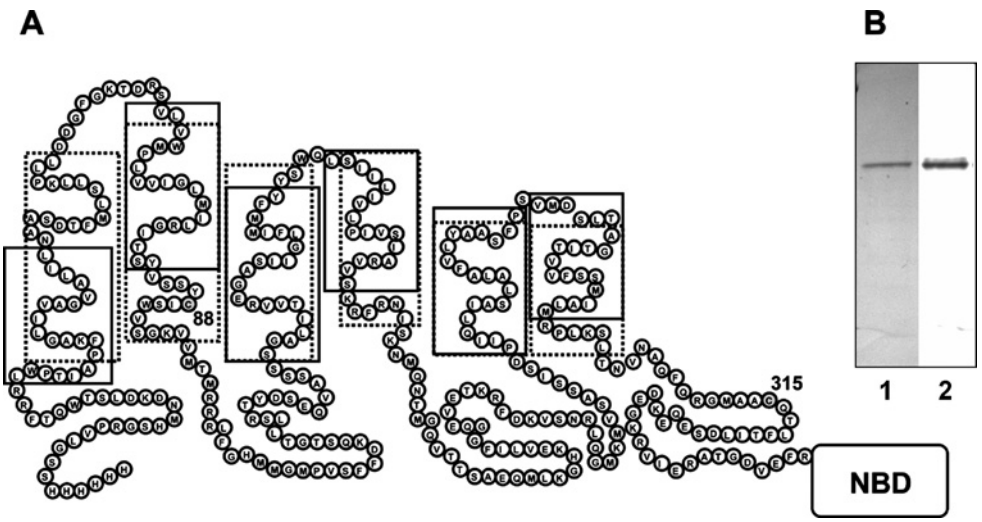

Figure 1 Topology and purification of MsbA

(**A**) Topological model of the MsbA protein. Each monomer contains 6 membrane-spanning helices forming a TM domain, with the NBD at the C-terminal end. Amino acid residues are indicated inside the circles; endogenous cysteine residues are numbered. The dotted box represents the TM domain boundaries of MsbA determined by EPR spectroscopy [21]. The X-ray crystal structure of *Salmonella typhimurium* MsbA (PDB: 3b60 [15]) suggests the following membrane-spanning domain boundaries: 1(27–52), 2(62–87), 3(142–163), 4(165–182), 5(248–271) and 6(283–305). The solid box represents the predicted TM domain boundaries (http://www.expasy.org/uniprot/P60752). (**B**) Purification of MsbA from cytoplasmic membrane vesicles of *E. coli* overexpressing the protein. Lane 1, SDS/PAGE analysis of purified MsbA (1 μg) in 0.05 % (w/v) DM, stained with Coomassie Blue; lane 2, Western blot of purified MsbA using an anti-His_6 antibody.

Additional structural information on MsbA comes from EPR spectroscopic studies [21–25]. Borbat et al. [25] recently proposed that a large change in the separation of the NBDs takes place during the dimerization–dissociation cycle of the *E. coli* protein. The available biochemical and dynamic information for this interesting protein is still very limited, and its transport substrates remain poorly defined. Among various biophysical methods for studying protein structure and dynamics, fluorescence spectroscopy is especially valuable for monitoring protein conformational changes induced by ligand binding. Recent work in our laboratory has employed the intrinsic Trp fluorescence of MsbA to characterize the binding of nucleotides and putative transport substrates, including lipid A [14]. Fluorescent probes targeted to Cys residues are also very useful, and have been used to study a variety of active transporters, including lactose permease, $MalFGK_2$, Pgp, the Ca^{2+}-ATPase and the Na^+/K^+-ATPase.

In the present study, we used purified MsbA labelled on Cys^{315} with the environmentally sensitive fluorescent probe MIANS [2-(4′-maleimidylanilino)naphthalene-6-sulfonic acid] [26,27]. Using fluorescence quenching, we observed simultaneous high affinity binding to MsbA of lipid A (the putative physiological substrate) and daunorubicin, which suggests that the protein has separate binding sites for these two compounds. The effects of nucleotide and lipid A/daunorubicin binding to MsbA were additive, and binding could occur in any order. The two substrate-binding sites appear to communicate with each other, and also with the nucleotide-binding site in the NBDs, as indicated by alterations in the binding affinity at one site when one of the others is occupied. Characterization of these substrate-binding processes is an essential first step towards understanding the catalytic/transport cycle of MsbA.

EXPERIMENTAL

Materials

Acrylamide, ammonium persulfate, Coomassie Brilliant Blue, and molecular mass standards were purchased from Bio-Rad Laboratories. PVDF electroblotting membrane was from Millipore. MIANS was purchased from Molecular Probes. The propafenone compound GP12 [28] was a gift from Dr Peter Chiba (Department of Medicinal Chemistry, University of Vienna, Austria). Other drugs and lipid A (diphosphoryl, from *E. coli* F583; Rd mutant) were obtained from Sigma-Aldrich. DM (*n*-dodecyl-β-D-maltoside) was purchased from Alexis Biochemicals. Egg PC (phosphatidylcholine) was purchased from Avanti Polar Lipids. Biobeads were supplied by Bio-Rad Laboratories. All other reagents were of analytical grade.

MsbA mutagenesis and expression

The pET28b vector (Novagen) containing the *msbA* gene with an N-terminal His_6 tag was described previously in [22]. Both native cysteine residues (Cys^{88} and Cys^{315}) were substituted with serine by site-directed mutagenesis using the QuikChange mutagenesis kit (Stratagene). For the substitution of Cys^{315} with serine, 3′-CGCGGTATGGCGGCTTCCCAGACGCTGTTTACCATT-5′ and 5′-AATGGTAAACAGCGTCTGGGAAGCCGCCATACC-GCG-3′ were used as the forward and reverse primers respectively. For the substitution of Cys^{88} with serine, the forward and reverse primers were 3′-ATGTCTCCAGCTACTCCATCTCCTGGGTA-TCAGGA-5′ and 5′-TCCTGATACCCAGGAGATGGAGTAGC-TGGAGACATA-3′ respectively. All primers were obtained from Invitrogen. Mutant plasmids were sequenced in full to verify the introduced mutations. The plasmids containing the wild-type and mutated *msbA* genes were transformed into BL21-Codonplus(DE3)-RIL competent cells (Stratagene). Cells cultured overnight at 37 °C in Luria–Bertani broth, supplemented with 30 μg/ml kanamycin, were used to inoculate a large-scale culture in fresh medium. Cells were grown at 37 °C until the attenuance (D_{600}) reached approx. 1, and MsbA overexpression was induced by the addition of 1 mM IPTG (isopropyl β-D-thiogalactoside). Growth was continued at 37 °C for 3 h, and cells were harvested by centrifugation at 7000 ***g*** for 15 min at 4 °C.

MsbA purification

Cell pellets were resuspended in 100 mM Hepes, 500 mM NaCl and 5 mM $MgCl_2$, pH 7.5, and passed through a French pressure cell disrupter at 1000 p.s.i. (1 p.s.i. = 6.9 kPa). Cell debris was removed by centrifugation at 15000 ***g*** for 20 min at 4 °C. For purification of His-tagged wild-type MsbA and mutants C88S and C315S, the resulting membranes were treated on ice with solubilization buffer [20 mM Hepes, 100 mM NaCl and 1.1 % (w/v) DM, pH 8.0] for 1 h. All further steps were carried out at 4 °C. Unsolubilized material was removed by ultracentrifugation (171500 ***g***, 30 min), and the supernatant was incubated for 1 h on ice with Ni-NTA (Ni^{2+}-nitrilotriacetate) agarose pre-equilibrated with buffer A [20 mM Hepes, 100 mM NaCl and 0.05 % (w/v) DM, pH 8.0] containing 10 mM imidazole. After incubation, the resin was packed into a column and contaminating proteins were washed off with buffer A and buffer B [20 mM Hepes, 100 mM NaCl and 0.05 % (w/v) DM, pH 7.0] containing 10 mM imidazole. When no further protein was detected in the flow-through (monitored at 280 nm), MsbA was eluted with buffer B supplemented with 250 mM imidazole. Fractions containing MsbA were pooled and concentrated to ~1 mg/ml. MsbA purity was monitored by SDS/PAGE analysis and Coomassie Blue staining, as well as by Western blotting after transfer to a nitrocellulose membrane. The blot was probed with mouse anti-His_6 antibody (Qiagen), followed by goat anti-mouse IgG-horseradish peroxidase conjugate, and bands were detected using the ECL® (enhanced chemiluminescence) detection system (Amersham).

MsbA was reconstituted into proteoliposomes using detergent destabilization [29]. Egg PC, at an initial molar ratio of 300 lipids per protein, was suspended in Hepes buffer (20 mM Hepes, 100 mM NaCl and 5 mM $MgCl_2$, pH 7.4) at a concentration of 4 mg/ml. The lipid suspension was extruded 11 times through a 400 nm polycarbonate filter (Whatman) using an extrusion device (Avestin). The liposome suspension was then titrated with a DM solution to a concentration of 0.15 % (w/v) and mixed with DM-solubilized concentrated MsbA (Centricon YM-50). The detergent-destabilized liposomes and purified protein were incubated for 30 min at 23 °C, Biobeads were added to a final concentration of 80 mg/ml, and the mixture was incubated for a further 1 h at 4 °C. After removal of the Biobeads, the proteoliposomes were pelleted by centrifugation (190000 ***g*** for 30 min at 4 °C). The proteoliposome protein concentration was measured using a modified Lowry assay [30]. The recovery of MsbA in the reconstituted proteoliposomes was ~85 %, and the ATPase activity of the proteoliposomes was increased by approx. 50 % following addition of a permeabilizing concentration of detergent (15 mM CHAPS). This suggests that ~2/3 of the reconstituted MsbA faces inwards (NBDs on the vesicle exterior), and ~1/3 faces outwards (NBDs in the vesicle lumen).

ATPase activity assay

Purified wild-type MsbA and the C88S and C315S mutants [~100 μg/ml in 0.05 % (w/v) DM] were assayed for ATPase activity using a colorimetric assay that measures the liberation of free P_i from ATP [31]. To determine the influence of various concentrations of ATP on MIANS-labelled MsbA, the ATPase activity was determined following labelling. Unreacted MIANS was quenched with 1 mM DTE (dithioerythritol) before measuring ATPase activity.

Site-specific MIANS labelling of MsbA

Purified MsbA (wild-type, MsbA-C88S and MsbA-C315S) was incubated with 10 μM MIANS for 2 h at room temperature (23 °C) in the dark. Unreacted MIANS was quenched with 1 mM DTE and the excess label was removed by dialysis overnight against Hepes buffer. The final concentration of MIANS-labelled MsbA used for fluorescence measurements was 100 μg/ml.

Fluorescence measurements

Fluorescence spectra were recorded at 23 °C using a PTI QuantaMaster C-61 steady-state fluorimeter (Photon Technology International). Emission spectra were recorded after excitation at 322 nm (4 nm slits). As a control, MIANS was reacted with DTE. To estimate the time needed for complete MIANS labelling of MsbA, 10 μM MIANS was added to the protein [100 μg/ml in 0.05 % (w/v) DM] and the reaction was followed continuously in real time at an emission wavelength of 420 nm. Intrinsic fluorescence spectra of MsbA and MsbA–MIANS were recorded with selective excitation of tryptophan residues at 290 nm, and also after denaturation of the proteins for 15 min at 90 °C with 6 M guanidine hydrochloride.

To determine how drugs and lipid A modulated MIANS labelling, 70 μg/ml MsbA in Hepes buffer containing 0.05 % (w/v) DM was preincubated with the test compound for 15 min at 23 °C. Each compound was used at a final concentration approx. 5-fold higher than its estimated K_d for binding to the protein, as determined by MIANS fluorescence quenching (see Table 2), to ensure that saturation was approached. Labelling was initiated by adding MIANS (20 μM) and fluorescence emission intensity at 420 nm was monitored continuously (0.2 s intervals), with excitation at 322 nm, for times up to 2000 s. Initial rates of labelling were measured from the linear rate of fluorescence intensity increase observed over the first 20 s after addition of MIANS.

Stoichiometry of MIANS labelling

Unlabelled and MIANS-labelled MsbA were transferred from high-salt to low-salt buffer using gel filtration chromatography on a 10 ml desalting column (Bio-Rad Laboratories). The samples were then lyophilized and redissolved in 6 M guanidine hydrochloride. The final protein concentration was determined using a modified Lowry assay [30] with bovine serum albumin as a standard, and adjusted to 350 μg/ml for both samples. The absorbance values from the protein assay were corrected for the presence of MIANS. The absorption spectra of both samples were recorded using a UV/visible spectrophotometer. To estimate the stoichiometry of labelling, the extinction coefficient of MIANS was taken as 27000 $cm^{-1} \cdot M^{-1}$ (Molecular Probes) and the molar mass of MsbA was assumed to be 65 kDa.

MS

MALDI–TOF (matrix-assisted laser-desorption ionization–time-of-flight) MS was used to determine which cysteine residues in MsbA were labelled by MIANS. Purified MsbA was digested with chymotrypsin (sequence grade; Roche Diagnostics) at 30 °C for 24 h, incubating 10 μg of protein per μg of protease in a 20 μl volume. MALDI–TOF was performed using a Bruker-Relex (Bruker-Franzen Analytik). The MIANS-labelling site of MsbA was identified by comparing the actual mass of the individual peptides from MALDI–TOF analysis with the predicted mass of the corresponding peptides obtained from the ExPASy peptide mass analysis tool (http://ca.expasy.org/tools/peptide-mass.html).

CD spectroscopy

Prior to CD measurements, unlabelled MsbA and MsbA–MIANS were transferred to phosphate buffer (10 mM phosphate and 100 mM NaF, pH 7.0) supplemented with 0.01 % (w/v) DM by

gel filtration on a 10 ml desalting column (Bio-Rad Laboratories). CD measurements were performed using a Jasco J-810 instrument equipped with an external water bath. The thermal stability of MsbA secondary structure was monitored by heating 350 μg/ml samples over the range 20–65 °C. The mean residue ellipticity was recorded at 5 °C intervals over the range 195–275 nm at a scanning rate of 100 nm/min. Four scans were accumulated at each temperature. The data pitch was 0.1 nm, the response time was 0.5 s and band width was 1 nm. CD spectra were corrected for the solvent CD signal recorded from 20–65 °C. Secondary structure analysis was carried out using the DICHROWEB server (http://www.cryst.bbk.ac.uk/cdweb/html/home.html).

Fluorescence quenching studies

Fluorescence quenching experiments with nucleotides (except ATP), drugs and lipid A were carried out at 23 °C using 250 μl of MsbA (100 μg/ml) in 100 mM Hepes, 50 mM NaCl, 5 mM $MgCl_2$ and 0.05 % (w/v) DM, pH 7.5. Experiments with ATP were carried out at 10 °C to prevent hydrolysis during the experiment. Working solutions were prepared in DMSO for drugs and in the 100 mM Hepes, 50 mM NaCl and 5 mM $MgCl_2$ buffer for nucleotides. Lipid A was resuspended at a concentration of 0.5 mg/ml (molecular weight 1.7–1.8 kDa) in 20 mM Hepes, pH 7.5. To quench the MIANS fluorescence, MsbA–MIANS samples were titrated with various substrates. After each addition, the samples were allowed to reach steady-state for 1 min and the fluorescence was measured at 420 nm. Fluorescence intensities were corrected for dilution, scattering, and the inner filter effect as described previously [32,33]. Fluorescence changes were routinely expressed as the percent change in fluorescence intensity at 420 nm induced by substrate relative to the intensity measured in the absence of substrate. Experimental data were computer-fitted to the following equation:

$$\left(\frac{\Delta F}{F_0}\right) \times 100 = \frac{(\Delta F_{max}/F_0 \times 100)[S]}{K_d + [S]}$$

where F_0 is the initial value of fluorescence intensity, ΔF is the change in fluorescence intensity at a given point in the titration, $(\Delta F/F_0 \times 100)$ is the percent quenching at substrate concentration $[S]$, $(\Delta F_{max}/F_o \times 100)$ is the maximal percent quenching and K_d is the dissociation constant. Fitting to a single-site model was carried out using nonlinear regression (Sigmaplot 10.0, Systat Software), and values for K_d and ΔF_{max} were estimated.

Double titration experiments were performed in essentially the same way, the only difference being that MsbA–MIANS was titrated first with one substrate, and then with a second. For lipid A/daunorubicin binding, as well as p[NH]ppA (adenosine 5′-[β,γ-imido]triphosphate)/lipid A or ATP/lipid A binding, the titrations were performed in each of two possible sequences. Each titration point was corrected for the inner filter effect, scattering, and dilution.

RESULTS

Purification of MsbA

Membrane vesicles were isolated from *E. coli* cells overexpressing His_6-tagged wild-type MsbA and the two site-directed mutants, C88S and C315S. After membrane solubilization in DM, MsbA purification was carried out using Ni-NTA chromatography. The fractions containing purified protein were pooled and concentrated, to yield approx. 1 mg of MsbA from 15 mg of membrane protein. Analysis using SDS/PAGE and Western blotting showed that MsbA was isolated at high purity (Figure 1B),

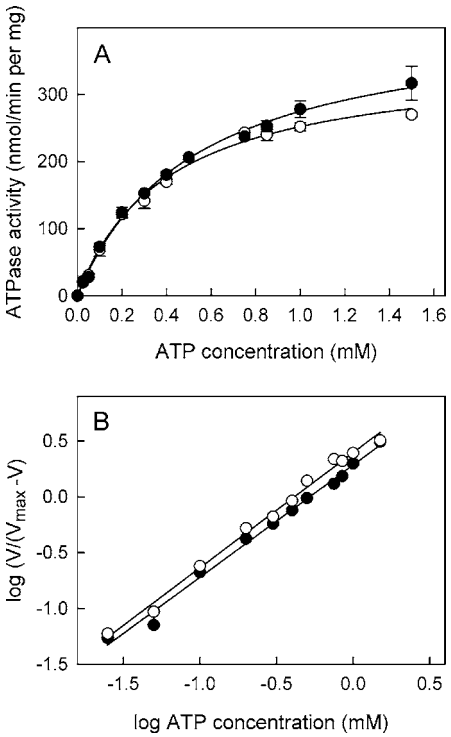

Figure 2 Catalytic activity of MsbA and MsbA–MIANS

(**A**) The ATPase activity at 37 °C as a function of ATP concentration for MsbA–MIANS (○) and unlabelled MsbA (●). Data points are the means ± S.D. ($n = 3$). In both cases, purified MsbA was in a buffer containing 0.05 % (w/v) DM. (**B**) Hill plot of the ATPase activity of wild-type MsbA (●) and MsbA–MIANS (○) as a function of ATP concentration; MsbA Hill coefficient, $n = 1.03 \pm 0.03$, MsbA–MIANS Hill coefficient, $n = 1.01 \pm 0.03$.

with an ATPase-specific activity of 400 ± 5 nmol/min per mg of protein (at 2 mM ATP) for wild-type protein. The ATPase activity of the C88S and C315S mutants did not differ substantially from that of wild-type MsbA. The ATPase activity of wild-type MsbA was measured for a range of ATP concentrations from 0.05–10 mM at 4, 23 and 37 °C (results for 37 °C are shown in Figure 2). Activity increased in a hyperbolic fashion with increasing ATP concentration, and levelled off above 1.5 mM ATP (Figure 2A). Similar ATPase activity dependence on ATP concentration was reported previously [4,7]. The K_m for unlabelled MsbA was 0.52 ± 0.04 mM, whereas for MIANS-labelled protein (see below) it was 0.41 ± 0.04 mM. The corresponding V_{max} values were 418 ± 12 and 354 ± 13 nmol/min per mg of protein, for unlabelled and MIANS-labelled MsbA respectively. We previously reported that purified MsbA is homodimeric in DM solution [14]. When the kinetic data for wild-type and MIANS-labelled MsbA were fitted to the Hill equation, coefficients close to 1 were obtained (Figure 2B), suggesting that the two monomers function independently, and do not interact co-operatively with each other. This is consistent with the "alternating sites" proposal of Senior et al. [34] for the mechanism of Pgp, which is also proposed to be a dual drug transporter and lipid flippase; only one NBD is thought to be active at any instant in time, and the two sites alternate in catalysis.

Site-specific labelling of MsbA with MIANS

MIANS has been widely used as a cysteine-reactive fluorescent probe for soluble and membrane-bound proteins. Its quantum yield and emission maximum are highly sensitive to the polarity of its local environment [26,27]. MsbA labelling was performed

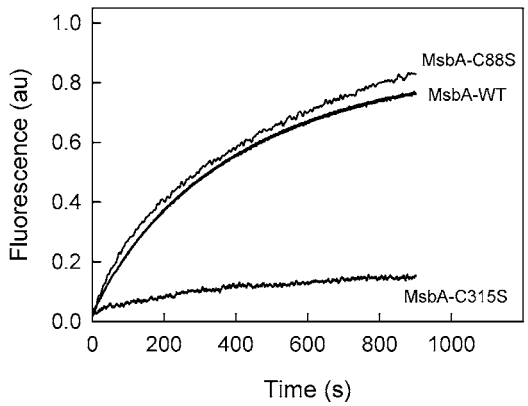

Figure 3 Reaction of wild-type and cysteine mutant MsbA proteins with MIANS

Time-dependent reaction of wild-type MsbA (MsbA-WT) and the site-directed mutants MsbA-C88S and MsbA-C316S with MIANS. MIANS labelling of MsbA (100 μg/ml) was carried out in buffer containing 0.05 % (w/v) DM. Labelling was initiated by addition of 10 μM MIANS, and fluorescence emission was recorded continuously at 420 nm ($\lambda_{ex} = 322$ nm).

under non-denaturing conditions with a 15-fold molar excess of the fluorophore, and yielded highly labelled protein after removal of free label by dialysis. As shown in Figure 1(A), MsbA has two native cysteine residues, one (Cys^{88}) at the cytoplasmic end of TM helix 2, and one (Cys^{315}) in the ICD connecting the C-terminal end of TM helix 6 to the NBD, as indicated by both EPR spectroscopy [21] and X-ray crystallography [15]. MsbA–MIANS retained an ATPase activity of 354 nmol/min per mg of protein (V_{max}) after labelling, approx. 15 % lower than native MsbA, indicating that activity is almost fully retained after labelling. The addition of 0.05–2 mM ATP did not protect MsbA from this small activity loss during labelling. This is perhaps not surprising, since both cysteine residues are expected to be distant from the ATP-binding site within the NBD (the catalytic site is located approx. 60 residues from Cys^{315} and 287 residues from Cys^{88}).

Stoichiometry of MIANS labelling

The calculated labelling stoichiometry was found to be approximately one MIANS molecule per one MsbA monomer, as estimated using the extinction coefficient of bound MIANS. One cysteine residue within each MsbA monomer could be modified with a labelling level of 100 %, but another possibility is that both cysteine residues are labelled, but to a lower extent. Partial labelling seems unlikely, since the molar ratio of label to protein is approx. 15:1, and MIANS is highly reactive. Cysteine residues within the TM regions of integral proteins are often highly resistant to labelling. For example, cysteine residues buried within the TM domain of Pgp were essentially completely inaccessible to covalent modification by MIANS [32]. We might expect Cys^{315} to be more readily labelled than Cys^{88}, which is located close to the membrane boundary at the cytoplasmic end of TM helix 2. MALDI–TOF experiments on unlabelled MsbA and MsbA–MIANS confirmed that this was indeed the case. The Cys^{315} residue of MsbA was fully modified with MIANS, since *m*/*z* of the QRGMAACQTLF peptide fragment increased from 1225.582 to 1641.438, and the difference in *m*/*z* of 416 corresponds to the molecular mass of MIANS (416.38 Da). MIANS labelling experiments were also carried out with site-directed mutants in which Cys^{88} and Cys^{315} were each replaced by serine. As shown in Figure 3, MsbA-C88S reacted with MIANS at the same rate and to a similar extent to the wild-type protein, whereas MsbA-C315S showed a very low background rate of reaction. These results confirm that Cys^{315} is the primary site of MIANS labelling in MsbA.

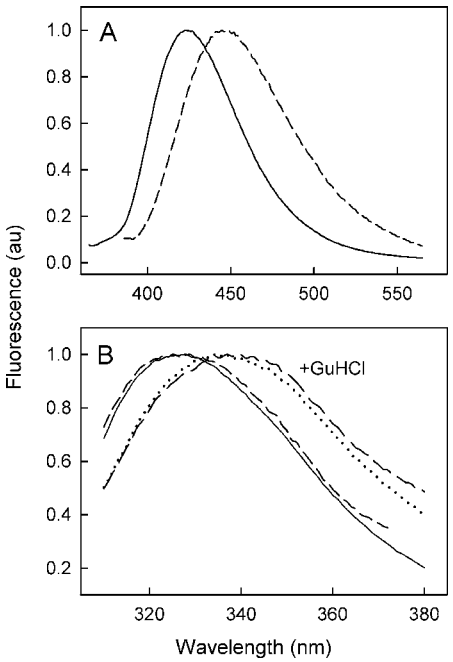

Figure 4 Fluorescence emission spectra of MsbA and MsbA–MIANS

(**A**) Fluorescence emission spectra of MIANS ($\lambda_{ex} = 322$ nm) covalently linked to MsbA (continuous line) and to the soluble compound DTE (broken line). (**B**) Intrinsic Trp fluorescence emission spectra ($\lambda_{ex} = 290$ nm) of MsbA–MIANS (short-dashed line and long-dashed line) and unlabelled MsbA (continuous line and dotted line) before and after, respectively, treatment with 6 M guanidine hydrochloride (GuHCl).

Fluorescence spectra of MsbA–MIANS

MIANS covalently linked to Cys^{315} in MsbA displayed an emission maximum, λ_{em}, of $\sim$423 nm, whereas the λ_{em} for MIANS following reaction with the soluble compound DTE was 448 nm (Figure 4A). This large blue shift of $\sim$25 nm indicates that Cys^{315} is located in a relatively nonpolar environment. The MsbA–MIANS fluorescence spectrum displayed a homogeneous shape, with the same spectral width as MIANS–DTE (Figure 4A), indicating that the labelled cysteine residues are located in a similar environment in the homodimer, as expected. The intrinsic tryptophan fluorescence spectrum of MsbA showed a λ_{em} of 328 nm (Figure 4B), which was substantially blue-shifted relative to the λ_{em} for the soluble Trp analogue, *N*-acetyltryptophanamide (356 nm; [35]). An almost identical tryptophan emission spectrum was observed for MsbA–MIANS. After heating with 6 M guanidine hydrochloride, both unlabelled MsbA and MsbA–MIANS displayed a substantial red shift in their emission maxima to 335 and 337 nm respectively, consistent with partial unfolding of the protein. Thus, MIANS-labelled MsbA behaves very similarly to the native protein, suggesting that its tertiary structure and folding are unaltered.

Secondary structure of MsbA

The CD spectra of native MsbA and MsbA–MIANS were essentially superimposable (Figure 5A), indicating that covalent linkage of MIANS does not perturb the overall protein secondary structure. Analysis of the CD spectrum using the DICHROWEB server [36] indicated that MsbA comprises 58 % α-helix, 9 %

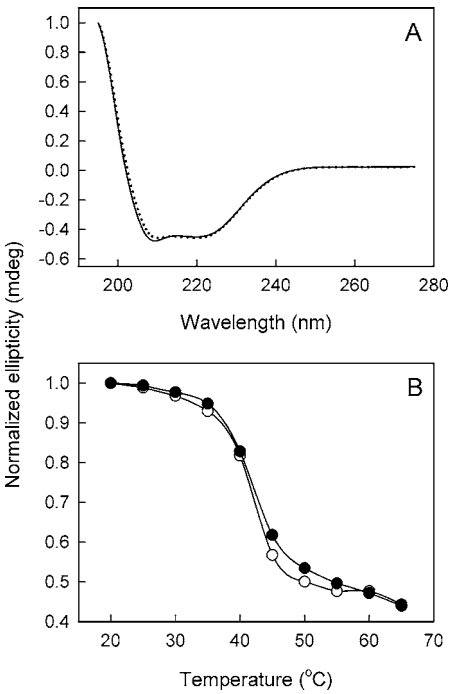

Figure 5 CD spectroscopy of MsbA and MsbA–MIANS

(**A**) CD spectra of unlabelled MsbA (continuous line) and MsbA–MIANS (dotted line) at a concentration of 0.35 mg/ml in buffer with 0.01 % (w/v) DM. (**B**) Thermal unfolding of MsbA and MsbA–MIANS monitored by CD spectroscopy. CD measurements were carried out on purified unlabelled MsbA (●) and MsbA–MIANS (○) at a concentration of 0.35 mg/ml in buffer with 0.01 % (w/v) DM. Molar ellipticity was recorded at 222 nm, which reports on α-helical unfolding.

β-strand and 34 % random coil/unassigned structure (8 % maximum error). These data are in good agreement with X-ray structures reported for MsbA from three bacterial species [15], where α-helices make up a large proportion of the secondary structure (63 % α-helix, 10 % β-strand; http://www.rcsb.org). The conformational stability of proteins can be assessed by thermal or chemical denaturation, which can be monitored by CD spectroscopy [37]. Thermal denaturation of native and MIANS-labelled MsbA resulted in CD spectral changes from 195–275 nm indicative of a coincident decrease in both secondary and tertiary structure. Figure 5(B) shows the temperature-induced CD change in MsbA at 222 nm, which was chosen because ellipticity changes at this wavelength reflect alterations in α-helical content [38]. The thermally-induced changes in secondary structure for both native and MIANS-labelled MsbA are essentially identical, showing that they unfold to the same extent, and with the same rate and temperature dependence. Thus, the folding and stability of MsbA is essentially unaltered after covalent attachment of MIANS.

Drugs and lipid A modulate MIANS labelling of MsbA

When MIANS reacts covalently with cysteine residues, it becomes highly fluorescent. We made use of this property to detect changes in labelling of MsbA upon binding of putative substrates, by following the reaction with MIANS in real time. Thus, addition of MIANS to purified MsbA led to a rapid increase in fluorescence emission intensity (Figure 6A). In the absence of substrates, MIANS labelling displayed the maximal rate (Figure 6A, trace 1) and complete labelling of MsbA was achieved in ~15 min at 23 °C. Such a fast reaction rate is typical when the -SH group is the target of MIANS labelling. When MsbA was preincubated before

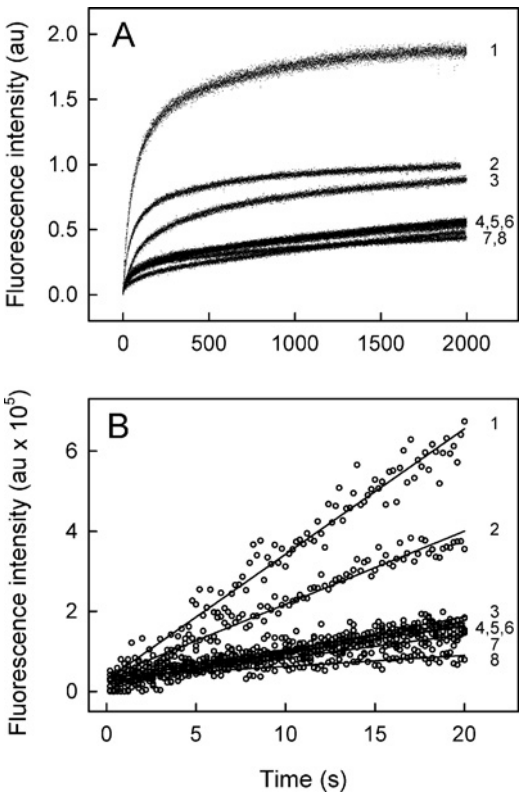

Figure 6 Rate of reaction of MsbA with MIANS in the presence of drugs and lipid A

MIANS labelling of MsbA (70 μg/ml) was carried out in buffer containing 0.05 % (w/v) DM. MsbA was preincubated for 15 min at 23 °C with various drugs and lipid A at concentrations (see Table 1) corresponding to ~5-fold higher than their K_d for binding (see Table 2). (**A**) Labelling was initiated by adding MIANS (20 μM) and fluorescence emission intensity fluorescence emission was recorded continuously (0.2 s intervals) at 420 nm ($\lambda_{ex} = 322$ nm), for times up to 2000 s. (**B**) Initial rates of labelling were observed over the first 20 s after addition of MIANS. 1, MsbA in the absence of drug; 2, 6 μM vinblastine; 3, 40 μM quercetin; 4, 6 μM verapamil; 5, 2 μM valinomycin; 6, 30 μM lipid A; 7, 4 μM propafenone GP12; and 8, 25 μM daunorubicin.

addition of MIANS with lipid A and various amphipathic drugs known to be substrates for MDR transporters, both the initial rate of increase in fluorescence (measured over the first 20 s) and the fluorescence intensity reached after 15 min were reduced, in some cases substantially (Figures 6A and 6B). Each drug was tested at an approximately saturating concentration (estimated as ~5-fold higher than the K_d for binding; see Tables 1 and 2). Of the drugs tested, the initial rate of MIANS labelling (measured over the first 20 s) was affected the least by vinblastine, and the most by daunorubicin (Figure 6B and Table 1). Determination of the extent of MIANS labelling of MsbA in the presence of each drug showed that the labelling efficiency was ~80 % or more in all cases (Table 1). Overall, these results suggest that binding of drugs and lipid A to MsbA appears to alter the accessibility or reactivity of Cys^{315} to labelling with the fluorophore.

Quenching of MsbA–MIANS by drugs and nucleotides

MIANS fluorescence quenching experiments were carried out on purified MsbA–MIANS in 0.05 % (w/v) DM buffer. Saturable concentration-dependent quenching of MsbA–MIANS fluorescence was observed on addition of several drugs, including valinomycin, vinblastine, verapamil, daunorubicin and quercetin (Figure 7), nucleotides (Figure 8), and the putative physiological

Table 1 Parameters for drug modulation of the rate of MsbA labelling by MIANS

Labelling experiments were carried out at 23 °C by adding MIANS (20 μM) to MsbA (70 μg/ml) in Hepes buffer containing 0.05 % (w/v) DM, in the absence or presence of various drugs. Fluorescence emission intensities were recorded continuously (every 0.2 s) for times up to 2000 s. Initial rates of labelling were measured from the linear rate of fluorescence intensity increase observed over the first 20 s after addition of MIANS. The labelling efficiency was determined after 2000 s by measuring the MIANS:MsbA stoichiometry.

Drug	Concentration (μM)	Initial rate of labelling (ms^{-1})	Labelling efficiency (%)
Control (none)		313 ± 6.3	105 ± 4.5
Vinblastine	6	182 ± 3.4	105 ± 4.5
Quercetin	40	85.0 ± 3.1	78.8 ± 1.0
Verapamil	6	71.0 ± 2.6	82.2 ± 3.6
Valinomycin	2	66.8 ± 3.4	101 ± 3.2
Lipid A	30	65.5 ± 2.5	118 ± 9.2
Propafenone GP12	4	59.1 ± 2.7	81.9 ± 4.2
Daunorubicin	25	27.4 ± 2.3	87.2 ± 1.3

Table 2 Parameters for fluorescence quenching of MsbA-MIANS by lipid A, drugs and nucleotides

Fluorescence quenching experiments with lipid A, drugs and nucleotides (except ATP) were carried out at 23 °C using MsbA (100 μg/ml) in Hepes buffer containing 0.05 % (w/v) DM. Corrected fluorescence emission intensities were fitted to a single binding-site model using non-linear regression, and values for K_d and ΔF_{max} were estimated. *Experiments using ATP were carried out at 10 °C to prevent hydrolysis of nucleotide.

Ligand	K_d (μM)	Maximal quenching ($\Delta F_{max}/F_0 \times 100$) (%)
Lipid A	5.46 ± 1.04	7.32 ± 0.49
Amphipathic drugs		
Valinomycin	0.35 ± 0.04	6.67 ± 0.11
Propafenone GP02	0.66 ± 0.14	7.04 ± 0.30
Vinblastine	1.20 ± 0.14	18.6 ± 0.50
Verapamil	1.26 ± 0.09	17.6 ± 0.30
Daunorubicin	4.60 ± 0.20	59.9 ± 4.4
Daunorubicin/egg PC	4.30 ± 0.79	60.0 ± 3.7
Quercetin	8.56 ± 0.79	56.0 ± 1.9
Nucleotides		
ATP*	3050 ± 430	10.9 ± 0.75
p[NH]ppA	470 ± 30	14.1 ± 0.30
ATP[S]	1.82 ± 0.29	6.01 ± 0.20
ADP	130 ± 60	8.48 ± 0.4
AMP	800 ± 200	7.84 ± 0.80

substrate, lipid A (Figure 9). The maximal percentage of quenching depended on the particular compound, and varied from 6 to 60 % (Table 2), with the highest quenching noted for daunorubicin and the lowest for ATP[S] (adenosine 5-[γ-thio]triphosphate). No significant shift in the λ_{em} for MsbA–MIANS was detected in the presence of any of these compounds. To examine MsbA interactions with drugs and nucleotides quantitatively, analysis of the fluorescence quenching titration experiments was carried out. For all drugs and nucleotides tested, the change in MIANS fluorescence followed a hyperbolic curve and was monophasic (Figures 7–9), which suggests the existence of only one binding site, or possibly two binding sites of similar affinity. Curve-fitting was used to estimate the dissociation constant, K_d, and the maximal percentage of quenching, ($\Delta F_{max}/F_o \times 100$), for each drug. The estimated K_d values obtained for amphipathic drugs ranged from 0.35 to 8.56 μM (Table 2), and are comparable with the affinity estimated for the physiological substrate, lipid A (5.46 μM). To test the effect of a lipid bilayer on MsbA drug binding affinity, the purified protein was reconstituted into egg PC

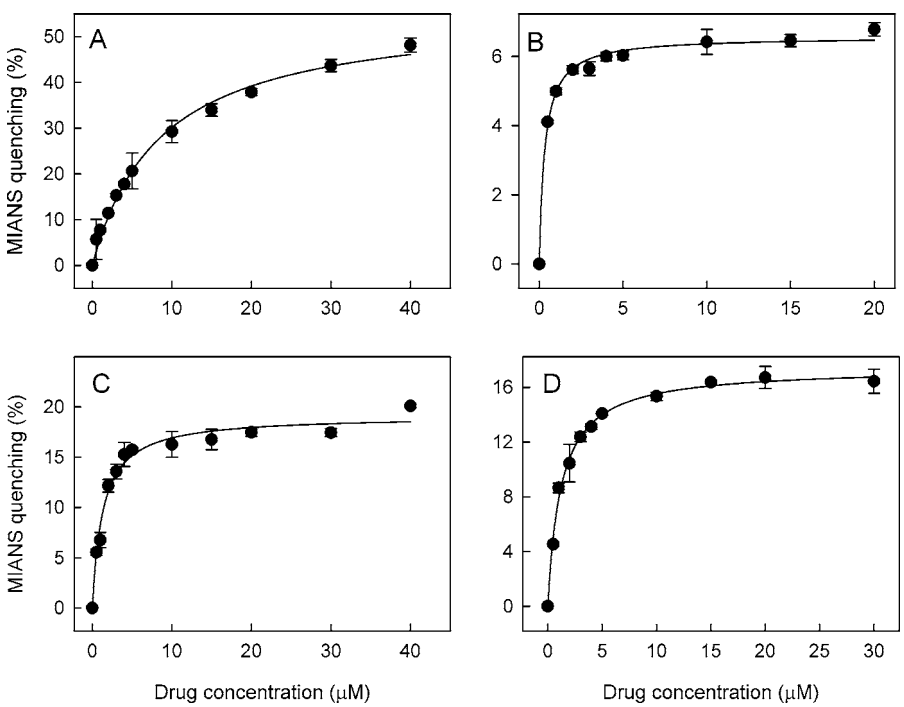

Figure 7 Quenching of MsbA–MIANS fluorescence by drugs

Increasing concentrations of various drugs were added to 100 μg/ml MsbA–MIANS in 0.05 % (w/v) DM buffer at 23 °C. The fluorescence emission was monitored at 420 nm ($\lambda_{ex} = 322$ nm). The percent quenching of MsbA–MIANS fluorescence ($\Delta F/F_0 \times 100$) was calculated relative to the fluorescence in the absence of drugs. The continuous line represents the best computer-generated fit of the data points to an equation describing interaction with a single type of binding site, and were used to estimate the K_d of binding. (**A**) quercetin, (**B**) valinomycin, (**C**) verapamil and (**D**) vinblastine. Data points are the means ± S.D. ($n = 3$).

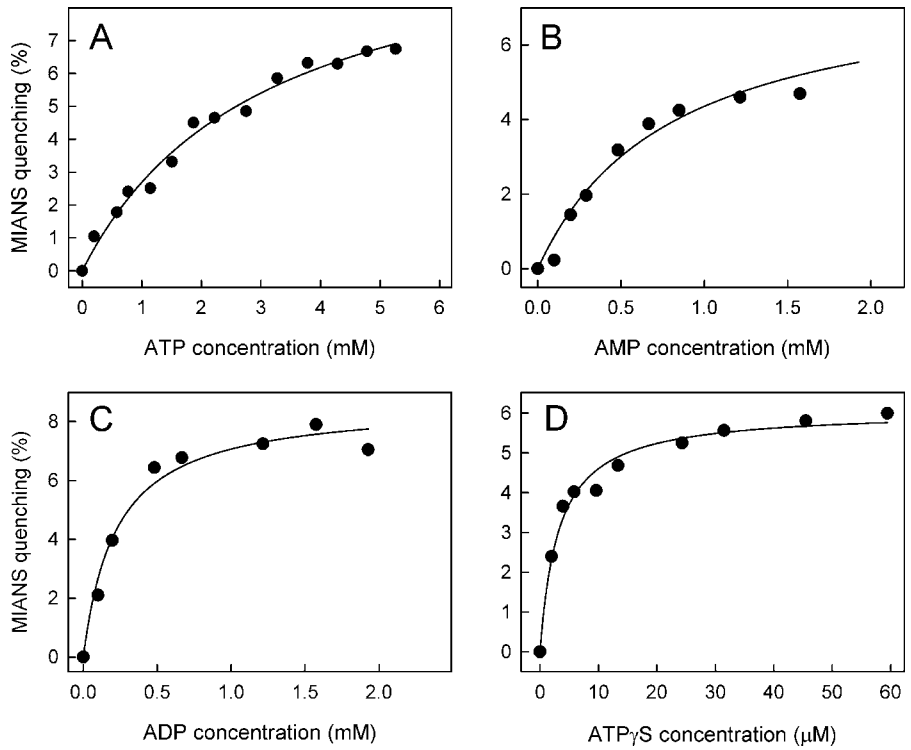

Figure 8 Quenching of MsbA–MIANS fluorescence by nucleotides

Increasing concentrations of nucleotides were added to 100 μg/ml MsbA–MIANS in 0.05 % (w/v) DM buffer at 23 °C (with exception of ATP, which was added to MsbA at 10 °C to prevent ATP hydrolysis). The fluorescence emission was monitored at 420 nm ($\lambda_{ex} = 322$ nm). The percent quenching of MsbA–MIANS fluorescence ($\Delta F/F_0 \times 100$) was calculated relative to the fluorescence in the absence of nucleotides. The continuous line represents the best computer-generated fit of the data points to an equation describing interaction with a single type of binding site, and were used to estimate the K_d of binding. (**A**) ATP, (**B**) AMP, (**C**) ADP and (**D**) ATP[S] (ATPγS). Data points are the means $\pm$ S.D. ($n = 3$).

proteoliposomes by detergent destabilization. The binding affinity of daunorubicin was essentially the same for MsbA in DM buffer and lipid bilayers (Table 2). The K_d for nucleotides varied from 0.13 to 3.5 mM, with the exception of ATP[S], which bound to MsbA with a relatively high affinity of 1.82 μM. ATP binding was measured at 10 °C to avoid hydrolysis of the nucleotide. At this temperature, the K_d of MsbA–MIANS for ATP binding was $>$ 7-fold higher than that determined for the non-hydrolysable analogue p[NH]ppA at 23 °C (Table 2).

Sequential binding of lipid A, daunorubicin and nucleotides to MsbA

To determine whether drug and lipid A molecules can bind to MsbA simultaneously, dual titration experiments were carried out, titrating the protein first with lipid A and then with daunorubicin. A separate experiment was then carried out with the same substrates, but titrating them in the reverse order. Figure 9(A) shows that MsbA–MIANS fluorescence can be quenched sequentially by lipid A and daunorubicin, implying that both of these molecules can bind to MsbA simultaneously at separate sites. The total MIANS quenching arising after binding of both lipid A and daunorubicin was approximately equal to the sum of the values observed for each species when added to MsbA separately, indicating that their effects on the protein are essentially additive. The percentage quenching values observed for lipid A and daunorubicin were also similar regardless of the order of titration. Interestingly, the binding affinity for lipid A was reduced $\sim$5-fold at 23 °C (K_d increased from 5.46 to 24.5 μM) and $\sim$7-fold at 10 °C (K_d increased from 2.44 to 18.1 μM) when the daunorubicin-binding site was occupied first (Table 3, Figure 9B). The ΔF_{max} for lipid A quenching also increased 2-fold when daunorubicin was bound first, indicating that conformational changes take place at the lipid A binding site when the drug-binding site is occupied. In contrast, pre-binding of lipid A did not affect the daunorubicin binding affinity at 23 °C, and led to only a small ($\sim$2-fold) reduction in affinity at 10 °C (Table 3, Figure 9A).

To determine if nucleotide binding at the NBD alters the binding affinity for lipid A (and vice versa), a dual titration experiment was performed with lipid A and ATP at 10 °C (to prevent ATP hydrolysis), and with lipid A and the non-hydrolysable analogue, p[NH]ppA, at 23 °C. Results showed that MsbA binding affinity for lipid A was reduced considerably, $\sim$8-fold, when ATP was pre-bound at 10 °C, and was $\sim$3-fold lower when p[NH]ppA was pre-bound at 23 °C (Table 3, Figure 9C). In contrast, the MsbA binding affinity for both ATP and p[NH]ppA was relatively unaffected by lipid A pre-binding (Table 3, Figure 9D). Similar results were obtained for binding of ATP with vinblastine or daunorubicin (results not shown). In each case, prior binding of nucleotide reduced the binding affinity of drug.

Dynamic quenching was used to determine the aqueous accessibility of MIANS within MsbA. This approach can also provide information on conformational changes taking place within the region close to the labelled cysteine residue following nucleotide and substrate binding [33]. Three collisional quenchers were employed; acrylamide (neutral), iodide ion (negative) and cesium ion (positive). Quenching of MsbA–MIANS was carried out in the presence of ATP and either lipid A or vinblastine, and compared with results obtained in the absence of drug or nucleotide. All the Stern–Volmer plots were linear, and no significant changes in the Stern–Volmer quenching constant, K_{SV}, were observed (results

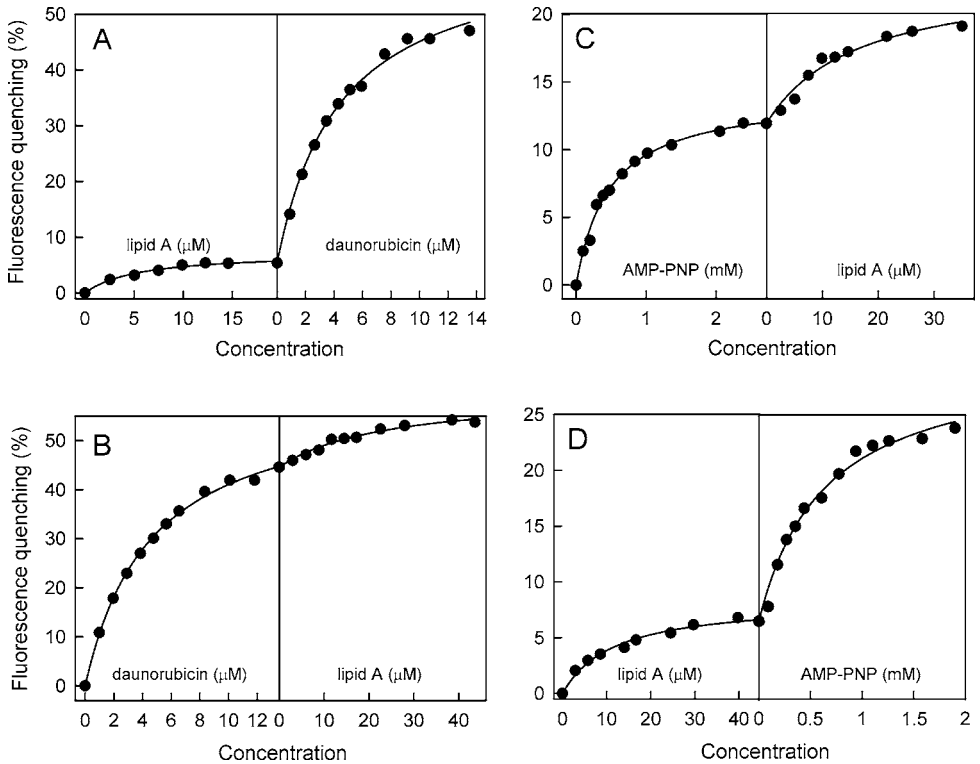

Figure 9 Sequential binding of lipid A, daunorubicin and nucleotides to MsbA

Dual sequential titrations of MsbA–MIANS in 0.05 % DM buffer with lipid A, daunorubicin and p[NH]ppA (AMP-PNP) were performed at 23 °C, with fluorescence emission monitored at 420 nm ($\lambda_{ex} = 322$ nm). Titration with (**A**) lipid A and then daunorubicin, (**B**) daunorubicin and then lipid A, (**C**) p[NH]ppA and then lipid A, (**D**) lipid A and then p[NH]ppA. The continuous lines represent the best computer-generated fit of the data points to an equation describing interaction with a single type of binding site, and were used to estimate the K_d of binding. Data points are the means of three experiments.

Table 3 Parameters for fluorescence quenching of MsbA–MIANS upon sequential binding of lipid A, daunorubicin and nucleotides

Dual titration experiments were performed at 23 °C or 10 °C (*) in which MsbA (100 μg/ml) in Hepes buffer containing 0.05 % (w/v) DM was titrated first with one substrate and then with a second, in each of two possible sequences. Corrected fluorescence intensities were fitted to a single binding-site model using non-linear regression and values for K_d and ΔF_{max} were estimated. [a]Data are taken from Table 2.

Ligand		K_d (μM)	Maximal quenching ($\Delta F_{max}/F_0 \times 100$) (%)
Lipid A		[a]5.46 ± 1.04	[a]7.32 ± 0.49
	after daunorubicin	24.5 ± 4.4	15.7 ± 1.4
	after p[NH]ppA	16.4 ± 3.7	10.9 ± 1.2
Lipid A*		2.44 ± 0.35	6.02 ± 0.11
	after daunorubicin*	18.1 ± 3.3	7.31 ± 0.50
	after ATP*	18.7 ± 3.3	17.7 ± 1.0
Daunorubicin		[a]4.60 ± 0.20	[a]59.9 ± 4.4
	after lipid A	4.42 ± 0.33	50.9 ± 1.5
Daunorubicin*		2.97 ± 0.23	60.6 ± 0.76
	after lipid A*	5.03 ± 0.11	63.8 ± 0.64
	after ATP*	9.59 ± 0.39	72.2 ± 1.5
ATP*		[a]3050 ± 430	[a]10.9 ± 0.75
	after lipid A*	2030 ± 300	12.0 ± 0.78
	after daunorubicin*	950 ± 230	5.45 ± 0.41
p[NH]ppA		[a]470 ± 30	[a]14.1 ± 0.3
	after lipid A	650 ± 80	23.2 ± 1.2

not shown), suggesting that the conformational rearrangements taking place following binding of ATP and substrates do not change the accessibility of the bound MIANS group.

DISCUSSION

More than 15 years have passed since MsbA first attracted attention as an essential *E. coli* transporter involved in the lipid A biosynthetic pathway [39]. However, there is still very limited biochemical and structural information available for this protein, which is generally considered to be a lipid A flippase. The inherent difficulty in purifying functionally-active membrane proteins in sufficient quantities for further analysis is partly responsible for this situation. Site-directed fluorescent labelling is a powerful approach to provide insights into the processes occurring in ABC proteins upon substrate binding and transport, as well as nucleotide binding and hydrolysis. Fluorescence spectroscopy is very sensitive, requiring only small amounts of material, and can provide information on both protein conformation and dynamics. The present study is the first to report site-specific fluorescent labelling of purified MsbA on a cysteine residue. CD thermal denaturation experiments and fluorescence spectra before and after denaturation revealed that MsbA–MIANS maintained its secondary structure and native folding. Purified His_6-tagged MsbA showed high ATPase activity that was retained following MIANS labelling. The small loss of MsbA ATPase activity upon MIANS labelling might arise from protein handling during the labelling procedure. On the other hand, the ICD containing Cys^{315} might be involved in transmitting a signal for transport between the NBD and the TM domain. Covalent modification of Cys^{315} could potentially influence interactions between the TM domain and the NBD, and in this way affect the intrinsic catalytic activity of the protein.

One MIANS group was incorporated per MsbA monomer, and experiments using site-directed mutations and MALDI–TOF

analysis indicated that of the two native cysteine residues, Cys^{315} was modified. The fluorescence emission spectrum of MsbA–MIANS displayed a single-component spectrum, with no evidence of broadening, suggesting that the MIANS-modified cysteine residues are in virtually identical local environments in the MsbA dimer, as expected from the crystal structure. Similar symmetry was noted for Pgp labelled with MIANS on cysteine residues within both NBDs [32]. The labelled Cys^{315} is located in the cytoplasmic extension of TM helix 6, within the ICD, and is predicted to be more accessible to solvent when compared with Cys^{88}, which is found in the middle of TM helix 2, close to the membrane boundary [15]. Utilizing a site-directed mutagenesis approach and accessibility measurements by EPR spectroscopy, Dong et al. [21] showed that TM helix 2 is in direct contact with the lipid bilayer. They found that the aqueous accessibility of residues in this helix is significant up to residue 82, but then gradually decreases [21]. TM helix 2 of MsbA in detergent solution is clearly highly shielded from reaction with MIANS, even in the absence of a membrane bilayer. Therefore, the region of the helix containing Cys^{88} is either protected by lipid/detergent molecules (if it faces the outer edge of the helix bundle), or is protected by other protein helices (if it does not). In contrast, the ICD and residues closest to the C-terminal end of helix 6 were proposed to have loose packing, since they displayed significant aqueous accessibility. Klug and co-workers also reported that an EPR probe linked to Cys^{315} was relatively mobile compared with other locations in the protein [22]. The fluorescent labelling pattern we obtained is consistent with this structural data.

The emission spectrum of MsbA–MIANS provides important information on the local environment of the modified Cys residue. The relatively large 25 nm blue shift observed when compared with MIANS–DTE suggests that Cys^{315} is located in a hydrophobic environment. A blue shift of similar magnitude was noted for MIANS-labelled cysteine residues in Pgp and lactose permease [32,40]. This nonpolar milieu might be provided by detergent molecules surrounding the protein or by the neighbouring helix residues of the ICD itself. Interestingly, when MsbA is aligned with its homologue, LmrA, Cys^{315} is located close to Glu^{314} of LmrA. This residue was also found to be located in a hydrophobic region within LmrA [41], which probably corresponds to the nonpolar environment we observe for MsbA.

The dimeric MsbA protein may transiently adopt an asymmetric conformation during the catalytic cycle, as proposed for Pgp [42], with one of the NBDs containing a tightly-bound (occluded) nucleotide, and the other a more loosely-bound nucleotide. However, the MIANS group is not located within the NBD itself, and it is not known whether the other domains of ABC proteins also develop asymmetry during ATP turnover. It should also be kept in mind that the asymmetric state of Pgp only appears to be formed under particular circumstances; during active ATP hydrolysis (transient), in catalytically inactive mutants in the presence of nucleotide, and in the presence of the non-hydrolysable ATP analogue, ATP[S] [43] (in the later two cases, it is a relatively stable "arrested" state). In the experiments we describe here, only drug binding is being observed; no nucleotide is added, and no catalytic turnover takes place, so we would not expect NBD asymmetry to develop.

Several drugs as well as lipid A greatly reduced the initial rate of labelling of MsbA with MIANS. Thus binding of substrates appears to alter the accessibility or reactivity of Cys^{315} to labelling with the fluorophore. This might be a direct effect of ligand binding (e.g. steric blocking) if Cys^{315} is located close to the drug-binding site, and the differences observed for the various drugs could reflect the fact that they interact with different sub-sites within a large flexible substrate-binding pocket. Alternatively, binding of substrates could induce a conformational change in MsbA, and thus indirectly alter the accessibility or reactivity of Cys^{315} to labelling by MIANS.

Titration of MsbA–MIANS with several drugs and lipid A resulted in saturable quenching, suggesting that these compounds bind to the protein. The estimated dissociation constants (Table 2) showed that drugs bound to MsbA with affinities in the range 0.35–9 μM; several bound with affinity comparable with that seen for lipid A. The binding affinities of MsbA for binding lipid A and vinblastine were previously determined by quenching of the intrinsic Trp fluorescence of the protein [14], and similar values were found to those estimated here from MIANS fluorescence quenching. Changes in MIANS fluorescence intensity and emission maximum following ligand binding can result from a direct effect when the fluorophore is situated very close to the binding site, or an indirect effect when conformational changes in other regions of the protein are transmitted to the fluorophore.

The Pgp drug-binding pocket was previously mapped to the interfacial zone of the cytoplasmic leaflet [44,45], which overlaps with the region where Cys^{315} is located. Cys^{315} may thus be positioned close to the site where drugs bind, explaining the high degree of fluorescence quenching by some compounds. Lipid A and certain drugs (e.g. verapamil and vinblastine) were reported to modulate MsbA ATPase activity [7,14], and more work will be needed to clarify the relationship between drug binding and ATPase activity. All drugs found to interact with MsbA in this study are known substrates of other MDR transporters, such as Pgp and LmrA, which recognize and transport a plethora of chemical species, many of which are positively charged. We titrated MsbA–MIANS with several negatively charged drugs; including the β-lactam antibiotic ampicillin, and the fluoroquinolone antibiotics, norfloxacin, ciprofloxacin and ofloxacin. No concentration-dependent quenching of MIANS fluorescence was observed, suggesting that these compounds do not interact with MsbA.

For Pgp, two drug-binding sites have been suggested based on cross-linking studies [46], biphasic quenching curves for some drugs [47] and dual fluorescence titrations [48]. The presence of two drug-binding sites was also proposed for LmrA [49]. The results of dual titration experiments using MsbA showed that lipid A and daunorubicin are capable of binding to the protein simultaneously, regardless of the order in which they are presented, implying that at least two distinct binding sites exist. Comparison of the binding affinities for lipid A and daunorubicin when the two compounds were presented to the protein in an ordered fashion indicated that the two binding sites engage in complex interactions with each other. Lipid A binding affinity is reduced almost 5-fold when it binds after daunorubicin. In contrast, the binding affinity for daunorubicin after pre-binding of lipid A is reduced only at 10 °C; no difference is seen at 23 °C. Thus lipid A binding affinity is negatively regulated by occupation of the other site by daunorubicin. Similar modulation of the binding affinity of one substrate by another during sequential binding was previously observed for Pgp [35,48,50]. Kimura et al. [51] proposed that the substrate-binding site of ABC proteins that are dual drug and lipid transporters is able to accommodate both a drug molecule and a cholesterol molecule, which they suggested might be involved in drug recognition. However, a recent study of cholesterol effects on Pgp-mediated drug binding and transport found no evidence to support this idea [52]. Our results do not distinguish between the two possibilities that lipid A and daunorubicin bind to unique allosterically linked sites, or to overlapping sub-sites within a large substrate-binding pocket. For Pgp, it has been proposed that TM helices from both halves of the protein form a large single drug-binding region which can accommodate multiple substrates by induced fit [53]. The existence of such a site explains the

broad substrate specificity of Pgp, and a similar concept may be applicable to MsbA, which also binds multiple substrates.

Transport mediated by ABC proteins is an energy-dependent event, during which conformational changes are transmitted between the NBDs and the TM domains. The precise order of the events that drive substrate transport is still under debate. Thus the ATP switch model proposes that the conformational changes associated with ATP binding are sufficient to switch the substrate-binding site from high to low affinity, thus releasing the substrate on the other side of the membrane [54]. Alternatively, ATP hydrolysis is the driving force for substrate transport [34]. The pump is re-set by either ATP hydrolysis or the exchange of ADP for ATP. The question of whether ATP binding is sufficient to trigger the high-affinity to low-affinity switch can be explored by analysing how ATP binding influences lipid A-binding affinity. Thus, in the sequential titration of MsbA with ATP or its non-hydrolysable analogue p[NH]ppA, and lipid A, it was been observed that the affinity of lipid A binding is reduced by only 3- to 8-fold when nucleotide is pre-bound, which is unlikely to be large enough to trigger dissociation of the lipid. Interestingly, a comparable reduction in lipid A binding affinity (4- to 7-fold) is observed when daunorubicin is bound first, suggesting that similar structural rearrangements may be taking place. We also observed that if ATP or p[NH]ppA bind after lipid A, their affinities are not substantially altered. Our results clearly show that binding of nucleotide and transport substrate to MsbA is not ordered.

Tombline et al. [42] reported that a single occluded ATP molecule is tightly bound in one NBD of the double catalytic carboxylate mutant of Pgp (E552A/E1197A). Recently, it has also been reported that binding of the non-hydrolysable ATP analogue, ATP[S], to Pgp promotes the formation of this occluded state [43]. The binding affinity of the occluded state of Pgp for ATP[S] is in the low μM range as measured by fluorescence quenching (A. Siarheyeva, R. Liu and F. J. Sharom, unpublished work), similar to that observed here for MsbA. It seems likely that the asymmetric occluded state, where the two NBDs display tight associations with a single nucleotide molecule, is a common feature in the catalytic pathway of MsbA and other ABC proteins. Since there are two MIANS groups per homodimer, the observed fluorescence signal will be an average of both of them. It is not currently known whether the other domains of ABC proteins also develop asymmetry during ATP turnover. If they do not, then it is unlikely that the spectral properties of the two MIANS probes in MsbA would reflect differences between the two monomers in the asymmetric state, since MIANS is located outside the NBDs. The occluded state of Pgp only appears to be formed under particular circumstances; during active ATP hydrolysis, in catalytically inactive mutants in the presence of nucleotide, and following binding of ATP[S]. In the experiments we describe in the present study, only drug and nucleotide binding is being observed and no catalytic turnover of nucleotide takes place, so we would not expect NBD asymmetry to develop in MsbA–MIANS.

The lipid A export system is a potential target for the development of novel antibiotics. Since MsbA is one of the rare transporters identified as being directly involved in the transport of lipid species, the identification of small molecules capable of interacting with this protein is of great importance. In addition to identifying drugs capable of interacting with MsbA, details of the conformational changes induced by ligand binding are also needed. The availability of purified, fluorescently labelled, catalytically active MsbA lays the groundwork for these types of studies. The results presented here and previously [14] strongly suggest that MsbA can bind multiple drugs, and may be both a lipid flippase and drug transporter. Thus MsbA may resemble other ABC proteins including LmrA [55], MRP1 (ABCC1) [56], Pgp [57,58], and its close relative MDR3 (ABCB4) [59], which function as both drug efflux pumps and outward translocators of membrane lipids. The mechanism by which drugs are extruded from cells may be closely related to lipid flippase activity, and lipid and drug translocation may take place through the same path [57,58,60]. It is possible that these proteins were originally involved in the transport of lipid derivatives, however during evolution they became engaged in the transport of other substrates sharing physicochemical properties with lipids, and in this way fulfilled an additional protective function in the cell.

ACKNOWLEDGEMENTS

We thank Dr. Candice Klug (Department of Biophysics, Medical College of Wisconsin, Milwaukee, WI, U.S.A.) for providing the pET28b plasmid.

FUNDING

F.J.S. is a Tier 1 Canada Research Chair in Membrane Protein Biology. This work was supported by a Discovery Grant from the Natural Sciences and Engineering Research Council of Canada (NSERC) and the Canada Research Chairs program.

REFERENCES

1 Dassa, E. and Bouige, P. (2001) The ABC of ABCs: a phylogenetic and functional classification of ABC systems in living organisms. Res. Microbiol. **152**, 211–229
2 Davidson, A. L. and Chen, J. (2004) ATP-binding cassette transporters in bacteria. Annu. Rev. Biochem. **73**, 241–268
3 Higgins, C. F. (2001) ABC transporters: physiology, structure and mechanism – an overview. Res. Microbiol. **152**, 205–210
4 Doerrler, W. T., Reedy, M. C. and Raetz, C. R. (2001) An *Escherichia coli* mutant defective in lipid export. J. Biol. Chem. **276**, 11461–11464
5 Doerrler, W. T., Gibbons, H. S. and Raetz, C. R. (2004) MsbA-dependent translocation of lipids across the inner membrane of *Escherichia coli*. J. Biol. Chem. **279**, 45102–45109
6 Zhou, Z. M., White, K. A., Polissi, A., Georgopoulos, C. and Raetz, C. R. (1998) Function of *Escherichia coli* MsbA, an essential ABC family transporter, in lipid A and phospholipid biosynthesis. J. Biol. Chem. **273**, 12466–12475
7 Doerrler, W. T. and Raetz, C. R. (2002) ATPase activity of the MsbA lipid flippase of *Escherichia coli*. J. Biol. Chem. **277**, 36697–36705
8 Tefsen, B., Bos, M. P., Beckers, F., Tommassen, J. and de Cock, H. (2005) MsbA is not required for phospholipid transport in *Neisseria meningitidis*. J. Biol. Chem. **280**, 35961–35966
9 Kol, M. A., Van Dalen, A., de Kroon, A. I. and de Kruijff, B. (2003) Translocation of phospholipids is facilitated by a subset of membrane-spanning proteins of the bacterial cytoplasmic membrane. J. Biol. Chem. **278**, 24586–24593
10 van Veen, H. W., Callaghan, R., Soceneantu, L., Sardini, A., Konings, W. N. and Higgins, C. F. (1998) A bacterial antibiotic-resistance gene that complements the human multidrug-resistance P-glycoprotein gene. Nature **391**, 291–295
11 van Veen, H. W., Venema, K., Bolhuis, H., Oussenko, I., Kok, J., Poolman, B., Driessen, A. J. and Konings, W. N. (1996) Multidrug resistance mediated by a bacterial homolog of the human multidrug transporter MDR1. Proc. Natl. Acad. Sci. U.S.A. **93**, 10668–10672
12 Reuter, G., Janvilisri, T., Venter, H., Shahi, S., Balakrishnan, L. and van Veen, H. W. (2003) The ATP binding cassette multidrug transporter LmrA and lipid transporter MsbA have overlapping substrate specificities. J. Biol. Chem. **278**, 35193–35198
13 Woebking, B., Reuter, G., Shilling, R. A., Velamakanni, S., Shahi, S., Venter, H., Balakrishnan, L. and van Veen, H. W. (2005) Drug-lipid A interactions on the *Escherichia coli* ABC transporter MsbA. J. Bacteriol. **187**, 6363–6369
14 Eckford, P. D. and Sharom, F. J. (2008) Functional characterization of *Escherichia coli* MsbA: interaction with nucleotides and substrates. J. Biol. Chem. **283**, 12840–12850
15 Ward, A., Reyes, C. L., Yu, J., Roth, C. B. and Chang, G. (2007) Flexibility in the ABC transporter MsbA: alternating access with a twist. Proc. Natl. Acad. Sci. U.S.A. **104**, 19005–19010
16 Smith, P. C., Karpowich, N., Millen, L., Moody, J. E., Rosen, J., Thomas, P. J. and Hunt, J. F. (2002) ATP binding to the motor domain from an ABC transporter drives formation of a nucleotide sandwich dimer. Mol. Cell **10**, 139–149
17 Zaitseva, J., Oswald, C., Jumpertz, T., Jenewein, S., Wiedenmann, A., Holland, I. B. and Schmitt, L. (2006) A structural analysis of asymmetry required for catalytic activity of an ABC-ATPase domain dimer. EMBO J. **25**, 3432–3443
18 Oldham, M. L., Khare, D., Quiocho, F. A., Davidson, A. L. and Chen, J. (2007) Crystal structure of a catalytic intermediate of the maltose transporter. Nature **450**, 515–521

19 Dawson, R. J. and Locher, K. P. (2007) Structure of the multidrug ABC transporter Sav1866 from *Staphylococcus aureus* in complex with AMP-PNP. FEBS Lett. **581**, 935–938
20 Dawson, R. J., Hollenstein, K. and Locher, K. P. (2007) Uptake or extrusion: crystal structures of full ABC transporters suggest a common mechanism. Mol. Microbiol. **65**, 250–257
21 Dong, J., Yang, G. and Mchaourab, H. S. (2005) Structural basis of energy transduction in the transport cycle of MsbA. Science **308**, 1023–1028
22 Buchaklian, A. H., Funk, A. L. and Klug, C. S. (2004) Resting state conformation of the MsbA homodimer as studied by site-directed spin labeling. Biochemistry **43**, 8600–8606
23 Buchaklian, A. H. and Klug, C. S. (2005) Characterization of the Walker A motif of MsbA using site-directed spin labeling electron paramagnetic resonance spectroscopy. Biochemistry **44**, 5503–5509
24 Buchaklian, A. H. and Klug, C. S. (2006) Characterization of the LSGGQ and H motifs from the *Escherichia coli* lipid A transporter MsbA. Biochemistry **45**, 12539–12546
25 Borbat, P. P., Surendhran, K., Bortolus, M., Zou, P., Freed, J. H. and Mchaourab, H. S. (2007) Conformational motion of the ABC transporter MsbA induced by ATP hydrolysis. PLoS. Biol. **5**, e271
26 Hiratsuka, T. (1992) Movement of Cys-697 in myosin ATPase associated with ATP hydrolysis. J. Biol. Chem. **267**, 14941–14948
27 Ksenzenko, M. Y., Kessel, D. H. and Rosen, B. P. (1993) Reaction of the ArsA adenosinetriphosphatase with 2-(4′-maleimidoanilino)naphthalene-6-sulfonic acid. Biochemistry **32**, 13362–13368
28 Tmej, C., Chiba, P., Huber, M., Richter, E., Hitzler, M., Schaper, K. J. and Ecker, G. (1998) A combined Hansch/Free-Wilson approach as predictive tool in QSAR studies on propafenone-type modulators of multidrug resistance. Arch. Pharm. (Weinheim) **331**, 233–240
29 Mason, A. J., Siarheyeva, A., Haase, W., Lorch, M., van Veen, H. and Glaubitz, C. (2004) Amino acid type selective isotope labelling of the multidrug ABC transporter LmrA for solid-state NMR studies. FEBS Lett. **568**, 117–121
30 Peterson, G. L. (1977) A simplification of the protein assay method of Lowry et al. which is more generally applicable. Anal. Biochem. **83**, 346–356
31 Sharom, F. J., Yu, X., Chu, J. W. K. and Doige, C. A. (1995) Characterization of the ATPase activity of P-glycoprotein from multidrug-resistant Chinese hamster ovary cells. Biochem. J. **308**, 381–390
32 Liu, R. and Sharom, F. J. (1996) Site-directed fluorescence labeling of P-glycoprotein on cysteine residues in the nucleotide binding domains. Biochemistry **35**, 11865–11873
33 Liu, R. and Sharom, F. J. (1997) Fluorescence studies on the nucleotide binding domains of the P-glycoprotein multidrug transporter. Biochemistry **36**, 2836–2843
34 Senior, A. E., al-Shawi, M. K. and Urbatsch, I. L. (1995) The catalytic cycle of P-glycoprotein. FEBS Lett. **377**, 285–289
35 Liu, R., Siemiarczuk, A. and Sharom, F. J. (2000) Intrinsic fluorescence of the P-glycoprotein multidrug transporter: Sensitivity of tryptophan residues to binding of drugs and nucleotides. Biochemistry **39**, 14927–14938
36 Lobley, A., Whitmore, L. and Wallace, B. A. (2002) DICHROWEB: an interactive website for the analysis of protein secondary structure from circular dichroism spectra. Bioinformatics **18**, 211–212
37 Piszczek, G., D'Auria, S., Staiano, M., Rossi, M. and Ginsburg, A. (2004) Conformational stability and domain coupling in D-glucose/D-galactose-binding protein from *Escherichia coli*. Biochem. J. **381**, 97–103
38 Wallace, B. A., Lees, J. G., Orry, A. J., Lobley, A. and Janes, R. W. (2003) Analyses of circular dichroism spectra of membrane proteins. Protein Sci. **12**, 875–884
39 Karow, M. and Georgopoulos, C. (1993) The essential *Escherichia coli* msbA gene, a multicopy suppressor of null mutations in the htrB gene, is related to the universally conserved family of ATP-dependent translocators. Mol. Microbiol. **7**, 69–79
40 Kwaw, I., Zen, K. C., Hu, Y. L. and Kaback, H. R. (2001) Site-directed sulfhydryl labeling of the lactose permease of *Escherichia coli*: helices IV and V that contain the major determinants for substrate binding. Biochemistry **40**, 10491–10499
41 Shilling, R., Federici, L., Walas, F., Venter, H., Velamakanni, S., Woebking, B., Balakrishnan, L., Luisi, B. and van Veen, H. W. (2005) A critical role of a carboxylate in proton conduction by the ATP-binding cassette multidrug transporter LmrA. FASEB J. **19**, 1698–1700
42 Tombline, G., Muharemagic, A., White, L. B. and Senior, A. E. (2005) Involvement of the "occluded nucleotide conformation" of P-glycoprotein in the catalytic pathway. Biochemistry **44**, 12879–12886
43 Sauna, Z. E., Kim, I. W., Nandigama, K., Kopp, S., Chiba, P. and Ambudkar, S. V. (2007) Catalytic cycle of ATP hydrolysis by P-glycoprotein: evidence for formation of the E.S reaction intermediate with ATP-γ-S, a nonhydrolyzable analogue of ATP. Biochemistry **46**, 13787–13799
44 Qu, Q. and Sharom, F. J. (2002) Proximity of bound Hoechst 33342 to the ATPase catalytic sites places the drug binding site of P-glycoprotein within the cytoplasmic membrane leaflet. Biochemistry **41**, 4744–4752
45 Lugo, M. R. and Sharom, F. J. (2005) Interaction of LDS-751 with P-glycoprotein and mapping of the location of the R drug binding site. Biochemistry **44**, 643–655
46 Loo, T. W., Bartlett, M. C. and Clarke, D. M. (2003) Simultaneous binding of two different drugs in the binding pocket of the human multidrug resistance P-glycoprotein. J. Biol. Chem. **278**, 39706–39710
47 Romsicki, Y. and Sharom, F. J. (1999) The membrane lipid environment modulates drug interactions with the P-glycoprotein multidrug transporter. Biochemistry **38**, 6887–6896
48 Lugo, M. R. and Sharom, F. J. (2005) Interaction of LDS-751 and rhodamine 123 with P-glycoprotein: evidence for simultaneous binding of both drugs. Biochemistry **44**, 14020–14029
49 van Veen, H. W., Higgins, C. F. and Konings, W. N. (2001) Multidrug transport by ATP binding cassette transporters: a proposed two-cylinder engine mechanism. Res. Microbiol. **152**, 365–374
50 Martin, C., Berridge, G., Higgins, C. F. and Callaghan, R. (1997) The multi-drug resistance reversal agent SR33557 and modulation of vinca alkaloid binding to P-glycoprotein by an allosteric interaction. Br. J. Pharmacol. **122**, 765–771
51 Kimura, Y., Kodan, A., Matsuo, M. and Ueda, K. (2007) Cholesterol fill-in model: mechanism for substrate recognition by ABC proteins. J Bioenerg. Biomembr. **39**, 447–452
52 Eckford, P. D. and Sharom, F. J. (2008) Interaction of the P-glycoprotein multidrug efflux pump with cholesterol: effects on ATPase activity, drug binding and transport. Biochemistry **47**, 13686–13698
53 Loo, T. W., Bartlett, M. C. and Clarke, D. M. (2003) Substrate-induced conformational, changes in the transmembrane segments of human P-glycoprotein – direct evidence for the substrate-induced fit mechanism for drug binding. J. Biol. Chem. **278**, 13603–13606
54 Higgins, C. F. and Linton, K. J. (2004) The ATP switch model for ABC transporters. Nat. Struct. Biol. **11**, 918–926
55 Margolles, A., Putman, M., van Veen, H. W. and Konings, W. N. (1999) The purified and functionally reconstituted multidrug transporter LmrA of *Lactococcus lactis* mediates the transbilayer movement of specific fluorescent phospholipids. Biochemistry **38**, 16298–16306
56 Kamp, D. and Haest, C. W. (1998) Evidence for a role of the multidrug resistance protein (MRP) in the outward translocation of NBD-phospholipids in the erythrocyte membrane. Biochim. Biophys. Acta **1372**, 91–101
57 Romsicki, Y. and Sharom, F. J. (2001) Phospholipid flippase activity of the reconstituted P-glycoprotein multidrug transporter. Biochemistry **40**, 6937–6947
58 Eckford, P. D. and Sharom, F. J. (2005) The reconstituted P-glycoprotein multidrug transporter is a flippase for glucosylceramide and other simple glycosphingolipids. Biochem. J. **389**, 517–526
59 Ruetz, S. and Gros, P. (1994) Phosphatidylcholine translocase: a physiological role for the mdr2 gene. Cell **77**, 1071–1081
60 Higgins, C. F. and Gottesman, M. M. (1992) Is the multidrug transporter a flippase? Trends Biochem. Sci. **17**, 18–21

Received 3 July 2008/18 December 2008; accepted 8 January 2009
Published as BJ Immediate Publication 8 January 2009, doi:10.1042/BJ20081364